

Correlated electrons in semiconductor quantum dots: Building an electron dimer molecule from the bottom-up

Achintya Singha,¹ Vittorio Pellegrini,^{1,*} Aron Pinczuk,² Loren N. Pfeiffer,³ Ken W. West,³ and Massimo Rontani^{4,†}

¹*NEST, Istituto di Nanoscienze – CNR and Scuola Normale Superiore, Pisa 56127, Italy*

²*Depts of Appl. Phys & Appl. Math. and of Physics, Columbia University, New York 10027, USA*

³*Department of Electrical Engineering, Princeton University, Princeton, NJ,
USA and Bell Laboratories, Alcatel-Lucent, Murray Hill, New Jersey 07974, USA*

⁴*S3, Istituto di Nanoscienze – CNR, Modena 41125, Italy*

(Dated: July 19, 2022)

We observe the low-lying collective excitations of a molecular dimer formed by two electrons in a GaAs semiconductor quantum dot in which the number of confined electrons is tuned by optical illumination. By employing inelastic light scattering we identify the inter-shell excitations in the one-electron regime and the distinct spin and charge modes in the interacting few-body configuration. In the case of two electrons a comparison with configuration-interaction calculations allows us to link the observed excitations with the breathing mode of the molecular dimer and to determine the singlet-triplet energy splitting.

PACS numbers: 73.21.La, 73.20.Qt, 73.43.Lp, 31.15.vn

The creation and control of electrons confined in semiconductor quantum dots (QDs) enables fundamental studies of Coulomb interaction at the nanoscale and allows to define optimal architectures for solid-state quantum information processing [1]. In the case of two electrons, singlet and triplet spin states with a well-defined energy splitting are under active investigation for the implementation of logic gates for quantum computing [1–3].

In the dilute limit of few electrons, a paradigm shift occurs as the liquid-like properties of the electrons – captured by a single-particle picture – cease to dominate and the impact of Coulomb correlation favors the formation of a molecular electron state with strong radial and angular order [4–9]. The molecular dimer formed by two electrons is especially relevant being the benchmark for the exploration of Coulomb correlation at the nanoscale. This state has been the subject of several theoretical investigations (e.g. [10–12]) albeit difficult to realize experimentally since it requires soft confinement potentials that are comparable to Coulomb interaction strengths. Two-electron correlated QDs were studied in magneto-transport experiments at finite fields [13].

Like in atomic nuclei [14], the emergence of strong correlation among the QD electrons manifests in the energetic structure of the low-lying collective modes that are accessible by inelastic light scattering [9, 15]. Optical investigations of the characteristic low-lying excitations of two electrons in the QD remain challenging. Such experiments are enabled by combining spectroscopy tools with charge tunability with single electron accuracy, as obtained in devices containing self-assembled InAs QDs [16, 17] where two-electron singlet and triplet states were observed by inelastic light scattering [18]. In these self-assembled QDs, however, the large confinement energy prevents the formation of a molecular dimer state.

In this Letter we report the identification of a dimer

molecular state of two electrons at zero magnetic field in nanofabricated GaAs/AlGaAs QDs. The evidence is found in the low-lying spin and charge excitations observed by resonant inelastic light scattering. Crucial to these experiments is the continuous charge tunability by photo-depletion that allows the creation of QDs with a selected number of electrons. We first identify the one-electron regime characterized by a single monopole excitation between Fock-Darwin (FD) levels —the states of the two-dimensional harmonic oscillator— that are simply linked to the in-plane confinement energy.

The observation of additional distinct spin and charge modes as electron numbers in the QDs are increased as we sweep the illumination intensity signals the emergence of a ground state composed by two and more interacting electrons. We show that the measured low-lying excitation mode energies are incompatible with a theoretical framework that neglects correlation effects. We propose an interpretation based on a configuration interaction (CI) approach (aka exact diagonalization) that precisely reproduces the inelastic light scattering spectra. In the case of two electrons the CI analysis reveals links between observed excitations and the breathing and center-of-mass oscillations and rigid-rotor rotations of the molecular electron dimer.

In the CI interpretation the rotation energies are $\hbar^2 M_{\text{rel}}^2 / 2I$, with I being the momentum of inertia and $M_{\text{rel}} = 0, \pm 1, \pm 2, \dots$ the angular momentum in the relative frame. To comply with the antisymmetry of the total two-electron wave function, M_{rel} must be even (odd) for a singlet (triplet) state. Therefore, the energy separation between the triplet and singlet ground states is the rotation quantum $\hbar^2 / 2I$, that as shown below is accessible by the inelastic light scattering experiments.

The sample is constructed as an array ($100 \mu\text{m} \times 100 \mu\text{m}$) of identical QDs (10^4 replica to improve the

signal-to-noise ratio displaying the same optical properties [19] and inter-dot spacing of $1 \mu\text{m}$). It is fabricated by electron beam lithography and inductively coupled-plasma reactive ion etching on a 25 nm wide, one-side modulation-doped $\text{Al}_{0.1}\text{Ga}_{0.9}\text{As}/\text{GaAs}$ quantum well. The measured low-temperature two-dimensional electron density and mobility are $1.1 \cdot 10^{11} \text{ cm}^{-2}$ and $2.7 \cdot 10^6 \text{ cm}^2/\text{Vs}$, respectively. Scanning electron microscope (SEM) images of such QDs are shown in Figs. 1(a) and (b).

The inelastic light scattering experiments were performed in a backscattering configuration ($q \leq 2 \cdot 10^4 \text{ cm}^{-1}$ where q is the wave-vector transferred into the lateral dimension) at $T = 2 \text{ K}$. A tunable ring-etalon Ti:Sapphire laser with a wavelength of 789 nm in resonance with the QD absorption (whose onset is at 813 nm) was focused on the QD array with a $100 \mu\text{m}$ diameter area, and the scattered light was collected into a triple grating spectrometer with CCD detection.

Photo-depletion of the QD electrons was achieved by continuous-wave HeNe laser excitation at 633 nm that creates electron-hole pairs in the AlGaAs barrier. Whereas the photoexcited electrons in the AlGaAs barrier contribute to charge compensation of the ionized donors, the photoexcited holes are swept in the QDs flattening the parabolic in-plane potential (i.e. decreasing the confinement energy $\hbar\omega_0$ and contributing to the removal of the confined electrons by electron-hole recombination [20, 21]) [cf. inset to Fig. 1(d)]. As shown below the method allows to fully photo-deplete the QDs and tune their population with single-electron accuracy by changing the HeNe laser intensity I_{HeNe} .

Distinct spin and charge intershell monopole modes (with $\Delta M = 0$, M is the total angular momentum) were detected as a function of I_{HeNe} by varying the linear polarization of the scattered photons [parallel (perpendicular) to that of the incoming laser for charge (spin)]. The condition of photo-depleted QDs (number of confined electrons $N = 0$) is defined by the absence of any inter-shell excitations. This is achieved at $I_{\text{HeNe}} = 1.82 \text{ W/cm}^2$ as displayed in Fig. 1(d). The $N = 1$ regime is characterized by a single excitation (degenerate in spin and charge) between FD levels with the same angular momentum at $2\hbar\omega_0$ ($\hbar\omega_0 = 1.1 \text{ meV}$), as shown in Fig. 1(c). This condition is reached at $I_{\text{HeNe}} = 1.46 \text{ W/cm}^2$. Peculiar to this regime is the absence of multiplets at higher energy, as confirmed by calculation of the light scattering cross section within a perturbative approach under the resonant conditions employed here [22].

Additional spin and charge modes appear at higher energy [see Figs. 2(a) and 4] as we further reduce I_{HeNe} . We identify the occurrence of two electrons in the QDs at the onset of these additional peaks at $I_{\text{HeNe}} = 0.68 \text{ W/cm}^2$. In this regime of shallow confinement, $\hbar\omega_0 \approx 1\text{--}2 \text{ meV}$, the electrons are highly correlated [6, 7, 9]. To identify the degree of correlation of the two electrons we theoret-

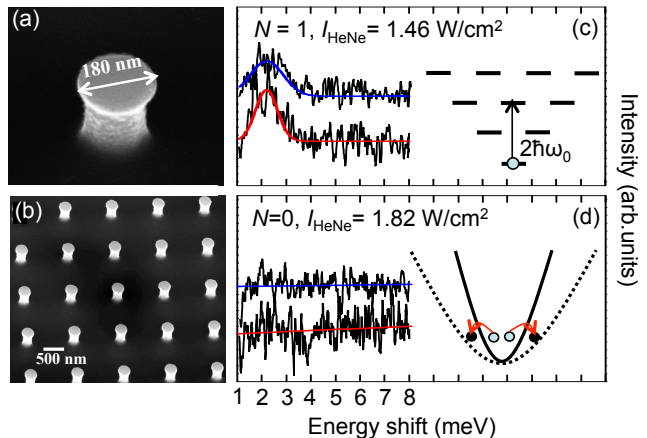


FIG. 1: (Color) (a) SEM images of a QD pillar and (b) of the QD array. (c) and (d) Resonant inelastic light scattering spectra of spin (fitted with red line) and charge (blue line) excitations for $N = 0$ and $N = 1$. The $N = 1$ intershell transition is shown in the inset to (c). The horizontal segments are the FD levels. The sketch of the QD in-plane parabolic potential is shown in the inset to (d). The photo-generated holes accumulate in the depletion region close to the physical borders of the etched pillar provoking a flattening of the confining potential (dotted curve). Removal of the electrons (filled light-blue circles) occurs via photo-recombination with the photo-excited holes (red arrows).

ically evaluate the spectra employing the full CI method [23]. This provides accurate energies and wave functions of strongly interacting systems, by building N -body states as linear combinations of many Slater determinants. The latter are obtained by filling with N electrons in all possible ways a truncated FD level basis set (here truncation includes the lowest 10 shells, with a relative error on excitation energies of $\approx 10^{-4}$). From CI wave functions of ground and excited N -body states we evaluate inelastic light scattering matrix elements and spectra [9, 15].

The spectra predicted by CI calculations for $N = 2$ [Fig. 2(b)] are remarkably similar to the experimental ones. In the evaluations the only free parameter, $\hbar\omega_0$, is adjusted to fit the energy of the four peaks shown in Fig. 2(a). The latter appear as two doublets —each formed by two peaks in the charge (blue lines) and spin (red lines) channels, labeled respectively as C_1, S_1 and C_2, S_2 in Fig. 2(b). Both spin excitations of Fig. 2(a) are slightly red shifted ($\approx 0.2 \text{ meV}$) from their charge counterparts. These splittings are also seen in the theoretical calculations in Fig. 2(b), which also reproduce the relative intensity of the peaks in each channel. The value of $\hbar\omega_0 = 1.6 \text{ meV}$ used in Fig. 2(b) is larger than that measured at $N = 1$, as expected for a lower I_{HeNe} [21].

The down triangles in Fig. 2(b) summarize instead the results of a self-consistent Hartree-Fock (HF) calculation [12] of spin and charge transition energies that neglects

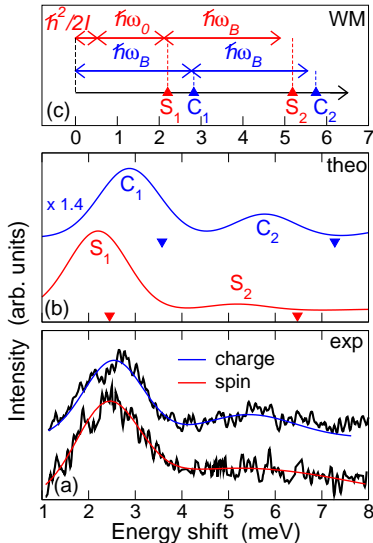


FIG. 2: (Color) (a) Experimental spectra (black lines) of spin and charge excitations at $I_{\text{HeNe}} = 0.68 \text{ W/cm}^2$. Red and blue lines are gaussian fits. (b) CI spectra for $N = 2$ (the peaks are artificially broadened by gaussians with FWHM = 1.5 meV). The down triangles point to the HF modes for $\hbar\omega_0 = 2.154 \text{ meV}$. (c) Comparison between CI (bottom energy axis) and WM modes (top and center energy axes for spin and charge excitations, respectively) with $\hbar\omega_0 = 1.6 \text{ meV}$.

correlation effects. This approach was extensively used to interpret previous light scattering spectra in the many-electron regime [24–26]. By fitting the position of S_1 [lowest down triangle in Fig. 2(b)] to its measured value [Fig. 2(a)] by properly tuning $\hbar\omega_0$, then the remaining three HF excitations are blue shifted more than 1 meV from their measured values. On the other hand, by fitting the position of the higher HF doublet (not shown) then S_1 is red shifted by $\approx 1 \text{ meV}$. This analysis therefore rules out an interpretation in terms of single-particle transitions between FD shells and establish the onset of electron correlation as we increase the electron population from $N = 1$ to $N = 2$.

The impact of Coulomb correlations is represented by the dimensionless radius r_s of the circle whose area is equal to the area per electron (in units of the Bohr radius [15]). For the CI calculation of Fig. 2(b) $r_s = 3.39$. In this dilute regime we expect the two electrons to form a molecule. This is confirmed in Fig. 2(c) by comparing the CI excitations of Fig. 2(b) (bottom energy axis) with the analytical predictions for a perfectly formed “Wigner” molecule [10] (WM) (top and middle axes for spin and charge excitations, respectively). The WM excitations have a composite nature: C_1 (C_2) is a single (double) excitation of the breathing mode, with energy

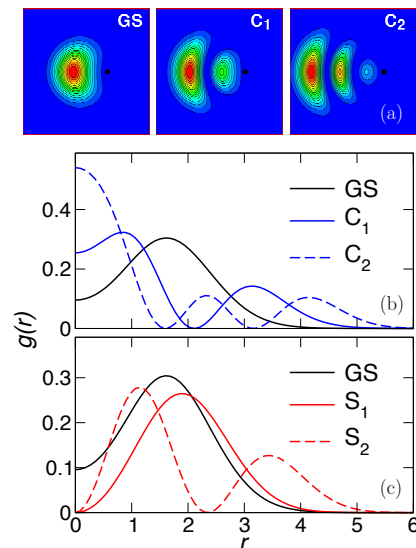


FIG. 3: (Color) Pair correlation functions for the CI states assigned in Fig. 2. The unit length is $\ell_{\text{QD}} = (\hbar/m^*\omega_0)^{1/2}$. (a) Conditional probability $P(x, y; x_0, y_0)$ of measuring an electron in the xy plane provided another one is fixed at position $(x_0, y_0 = 0)$, labelled by a black dot, where x_0 is located at the average value of r . From left to right: ground (GS) and excited states C_1 and C_2 , respectively. The squares’ size is 7×7 , and the 15 equally spaced contour levels go from blue (minimum) to red (maximum). (b-c) Pair correlation functions $g(r)$ vs r for the ground state, charge (b), and spin (c) excitations, respectively.

$\hbar\omega_B$ ($2\hbar\omega_B$), S_1 is a dipolar center-of-mass excitation $\hbar\omega_0$ plus a rotational quantum $\hbar^2/2I$ (the system as a whole keeps $M = 0$), and S_2 adds a breathing mode quantum. The agreement between CI and WM predictions in Fig. 2(c) is very good, with small deviations only for the higher excitations. Remarkably, spin and charge excitations scale differently with $\hbar\omega_0$, since $\omega_B = \sqrt{3}\omega_0$ whereas $I \propto \omega_0^{-4/3}$. The WM estimate for $\hbar^2/2I$, and hence the singlet-triplet splitting, is 0.517 meV.

In Fig. 3(a) we plot the conditional probability $P(x, y; x_0, y_0)$ of finding an electron at position (x, y) provided the other one is fixed at (x_0, y_0) (black dot). In the ground state (GS, left panel) the well developed correlation hole around the fixed electron suggests the freezing of the relative distance r . This is best seen from the pair correlation function $g(r)$ [black line in Fig. 3(b)], which for $N = 2$ is the square modulus of the relative-motion wave function. Since $g(r)$ is the probability that two electrons are at distance r , its well developed maximum around $r \approx 1.5$ [in units of the characteristic QD length $\ell_{\text{QD}} = (\hbar/m^*\omega_0)^{1/2}$] identifies the inter-electron equilibrium distance of the molecule. Besides, the plots of C_1 and C_2 in Fig. 3(a) [Fig. 3(b)] show respectively one and two additional nodal surfaces in the xy plane (nodes along r), pointing to the excitation of respectively one

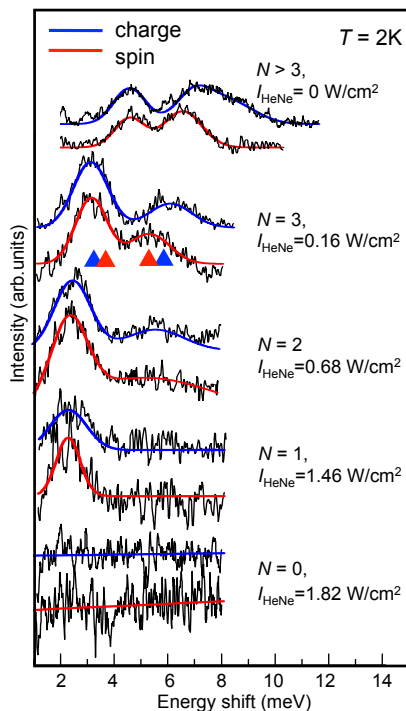


FIG. 4: (Color) Evolution of spin and charge excitations as a function of I_{HeNe} . Curves are best-fits to the data with zero, one or two gaussians. Up triangles point to the CI energies of spin (red) and charge (blue) modes.

and two quanta of the breathing mode. Note that the molecule is not perfectly formed due to residual electron delocalization [$g(r=0) \neq 0$ in Fig. 3(b)]. Spin excitations [red lines in Fig. 3(c)] have a different nature: $g(r=0) = 0$ for symmetry [$g(r) \propto r^{M_{\text{rel}}}$ as $r \rightarrow 0$ and $M_{\text{rel}} = 1$] and S_1 (S_2) has no node (one node) at finite r , consistently with the the excitation of no (one) breathing mode quantum. A similar analysis in the center-of-mass coordinates (not shown) confirms all the assignments of Fig. 2(c).

Figure 4 summarizes the evolution of the collective excitations as a function of I_{HeNe} . The blue shift of the modes manifests the increase of $\hbar\omega_0$ at lower I_{HeNe} , whereas the absence of a significant splitting of the two low-lying spin and charge modes for $I_{\text{HeNe}} < 0.68 \text{ W/cm}^2$ indicates a renormalization of their energies due to the increment of N [27]. Indeed the spectra at $I_{\text{HeNe}} = 0.16 \text{ W/cm}^2$ agree well with the CI excitation energies for $N = 3$, shown as up triangles in Fig. 4. The best agreement with the experimental data is obtained with $r_s = 2.18$ ($\hbar\omega_0 = 2.8 \text{ meV}$), a value significantly smaller than the one for $N = 2$. This decrease of r_s weakens electron correlations and it stops at $I_{\text{HeNe}} = 0$. Then the spectra resemble those obtained in similar QDs studied previously by us [9, 15] and interpreted as due to the low-lying collective spin and charge excitations of $N > 3$

electrons with $r_s \approx 2$.

In conclusion, we have reported the characteristic excitations of two correlated electrons (a molecular dimer) in nanofabricated GaAs quantum dots. Charge tunability with single electron accuracy is obtained by photodepletion. These studies open new opportunities for understanding the ground states of few electrons in semiconductor quantum dots in the regime of strong Coulomb interaction and weak confinement potential.

V. P. and M. R. are supported by the projects MIUR-PRIN 2008H9ZAZR and INFN-CINECA 2009. A. P. is supported by the NSF Nanoscale Science and Engineering Initiative Award No. CHE-0641523, by the NSF Grants No. DMR-0352738 and DMR-0803445, by the DOE Grant No. DE-AIO2-04ER46133, and by a grant from the W. M. Keck Foundation. We thank E. Molinari and G. Goldoni for helpful discussions.

* Electronic address: vp@sns.it

† Electronic address: rontani@unimore.it

- [1] R. Hanson *et al.*, Rev. Mod. Phys. **79**, 1217 (2007).
- [2] G. Burkard, D. Loss, D. P. DiVincenzo, Phys. Rev. B **59**, 2070 (1999).
- [3] D. M. Zumbühl *et al.*, Phys. Rev. Lett. **93**, 256801 (2004).
- [4] G. W. Bryant, Phys. Rev. Lett. **59**, 1140 (1987).
- [5] P. A. Maksym and T. Chakraborty, Phys. Rev. Lett. **65**, 108 (1990).
- [6] R. Egger *et al.*, Phys. Rev. Lett. **82**, 3320 (1999).
- [7] S. M. Reimann, M. Koskinen, and M. Manninen, Phys. Rev. B **62**, 8108 (2000).
- [8] A. Ghosal *et al.*, Nature Phys. **2**, 336 (2006).
- [9] S. Kalliakos *et al.*, Nature Phys. **4**, 467 (2008).
- [10] C. Yannouleas and U. Landman, Phys. Rev. Lett. **85**, 1726 (2000); A. Matulis and F. M. Peeters, Solid State Commun. **117**, 655 (2001).
- [11] U. Merkt, J. Huser, and M. Wagner, Phys. Rev. B **43**, 7320 (1991); D. Pfannkuche, V. Gudmundsson, and P. A. Maksym, Phys. Rev. B **47**, 2244 (1993).
- [12] M. Rontani *et al.*, Phys. Rev. B **59**, 10165 (1999).
- [13] C. Ellenberger *et al.*, Phys. Rev. Lett. **96**, 126806 (2006).
- [14] B. R. Mottelson, Rev. Mod. Phys. **29**, 2 (1957).
- [15] C. P. Garcia *et al.*, Phys. Rev. Lett. **95**, 266806 (2005).
- [16] H. Drexler *et al.*, Phys. Rev. Lett. **73**, 2252 (1994).
- [17] T. Brocke *et al.*, Phys. Rev. Lett. **91**, 257401 (2003).
- [18] T. Köppen *et al.*, Phys. Rev. Lett. **103**, 037402 (2009).
- [19] S. Kalliakos *et al.*, Appl. Phys. Lett. **90**, 181902 (2007).
- [20] I. V. Kukushkin, Phys. Rev. B **40**, 4179 (1989).
- [21] S. Kalliakos *et al.*, Nano Lett. **8**, 577, (2008).
- [22] C. Steinebach, C. Schüller, and D. Heitmann, Phys. Rev. B **59**, 10240 (1999).
- [23] M. Rontani *et al.*, J. Chem. Phys. **124**, 124102 (2006).
- [24] R. Strenz *et al.*, Phys. Rev. Lett. **73**, 3022 (1994).
- [25] D. Lockwood *et al.*, Phys. Rev. Lett. **77**, 354 (1996).
- [26] C. Schüller *et al.*, Phys. Rev. Lett. **80**, 2673 (1998).
- [27] In fact, according to CI calculations, this splitting should increase with $\hbar\omega_0$ when $N = 2$.